The modulation to Cerenkov second-harmonic in a $LiTaO_3$ waveguide with annular poling domain

2016 J. Opt. 18 015503

(http://iopscience.iop.org/2040-8986/18/1/015503)

IOP Publishing

Journal of Optics

J. Opt. 18 (2016) 015503 (5pp)

doi:10.1088/2040-8978/18/1/015503

The modulation to Cerenkov second-harmonic in a $LiTaO_3$ waveguide with annular poling domain

C D Chen[1] and X P Hu[2]

[1] College of Science, Nanjing University of Aeronautics and Astronautics, Nanjing 211100, People's Republic of China
[2] National Laboratory of Solid State Microstructures, Nanjing University, Nanjing 210093, People's Republic of China

E-mail: cdchen@nuaa.edu.cn

Received 10 August 2015, revised 13 October 2015
Accepted for publication 14 October 2015
Published 20 November 2015

Abstract

We report the modulated Cerenkov up-conversion in a $LiTaO_3$ waveguide with an annular domain structure. As a result of the continuous rotational symmetry of such a structure, the phase velocity of the nonlinear polarization wave has a wide modulation tolerance. The reciprocal vectors which could be involved in the interaction had a threshold range associated with the waveguide parameters. The experimental results and simulations demonstrated that the radiation intensity had a close relationship with the overlap between the pump and the radiated wave, which could be decreased by non-collinear reciprocal vectors. Our detailed discussions on the Cerenkov frequency-doubling process using such an annular-poling crystal may lay the groundwork for the further study of the modulation of other nonlinear Cerenkov processes.

Keywords: second-harmonic generation, optical waveguide, nonlinear Cerenkov radiation

(Some figures may appear in colour only in the online journal)

1. Introduction

Cerenkov second harmonic generation (SHG) is a well-known parametric process in optical waveguides or nonlinear photonic crystals (NPCs) via a second-order nonlinear interaction [1–9]. It occurs when the nonlinear polarization wave in a waveguide has a faster phase velocity ($\vec{v}_p$) than that of a free wave at the harmonic ($\vec{v}'$) in the material, such as $LiNbO_3$ or $LiTaO_3$ crystals. Since the concept of quasi-phase-matching (QPM) was brought forward [10], QPM Cerenkov up-conversion [11–13] and nonlinear diffraction [14] have been widely studied. By means of QPM technology, the poling domain structure could provide different reciprocal vectors to modulate $\vec{v}_p$ of the nonlinear polarization wave. With QPM technology extending from one dimension (1D) to two dimensions (2D), 2D NPCs have aroused much more interest recently. Various optical effects have been discovered up to now, such as conical SHG [15], nonlinear conical diffraction [16–18], Cerenkov-type SHG [19–22], Cerenkov difference frequency generation [23], omni-directional phase-matching [24] and so on.

Compared with a 2D NPC with square, rectangular or hexagonal symmetry, it is particularly the one with an annular modulation of $\chi^{(2)}$ that could provide many non-collinear reciprocal vectors with a continuous circular distribution [25, 26]. Most previous investigations of Cerenkov radiation mainly focused on 1D QPM or non-QPM waveguides. If Cerenkov SHG takes place in annular poled NPC waveguides, $\vec{v}_p$ of the nonlinear polarization wave could be equally modulated within a much greater tuning range than that of a 1D NPC, and the corresponding Cerenkov radiation will be emitted in different spatial directions. In contrast to the extremely strict phase-matching requirement in waveguide SHG between discrete guided modes, the fundamental guided mode and the frequency up-converted radiated mode can be automatically satisfied solely by adjusting the waveguide parameters through the Cerenkov scheme. Up to now, there have been no detailed reports on Cerenkov radiation in a nonlinear annular poled waveguide.

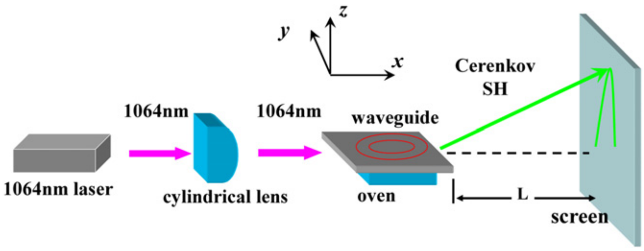

Figure 1. A schematic diagram of the experimental setup.

In this paper, we present experimental and numerical results for the modulation of Cerenkov SHG in an annular periodic-poled $LiTaO_3$ waveguide. When the fundamental beam passed through nearly the center of its domain structure, reciprocal vectors with distinct orientations would result in different SHG spot positions and intensities on the screen.

2. Experimental setup

In the experiment, a z-cut $LiTaO_3$ (LT) wafer of 0.5 mm thickness was first annular periodically poled using the electrical poling technique at room temperature, which formed a domain period of $\Lambda = 7\ \mu$m and a diameter of about 4 mm. Then the poled sample was proton-exchanged in benzoic acid for 6 h at 220 °C and subjected to annealing treatment for 5 h at 380 °C, which could recover the nonlinear coefficient and create a graded-index layer in the waveguide region. The thickness of the formed waveguide layer is about 3.9 μm, and the effective refractive index of the fundamental mode is about 2.1641 at a wavelength of 1064 nm. The end-faces of the waveguide were polished for our optical measurements.

A schematic of the experimental setup is shown in figure 1. As a fundamental source in our experiment, we used a side-pumped Q-switched Nd:YAG laser operating at 1064 nm with a pulse width of ~50 ns. The pulse repetition rate was set to be 5 kHz and the z-polarized 1064 nm was focused onto the NPC waveguide by a cylindrical lens with a focal length of 5 mm. The focused beam size was about 1.1 mm (y-axis) $\times$ 4 μm (z-axis). A screen was placed about 40 mm away from the output facet of the sample for the projection of generated radiation. The waveguide was kept at room temperature (about 30 °C) by use of an oven.

3. Experimental results and discussion

The fundamental power in our experiment was set to be 500 mW and focused passing through the center of our sample, as shown in figure 2(a). Under such circumstances, all of the available reciprocal vectors provided by the annular domain geometry could participate in Cerenkov SHG, as shown in figure 2(b). The phase-matching condition can be written as:

$$\left|\vec{\beta}_\omega + \vec{\beta}_\omega + \vec{G}_{\alpha(-\alpha)}\right| = |\vec{k}_{2\omega}| \cos\theta, \tag{1}$$

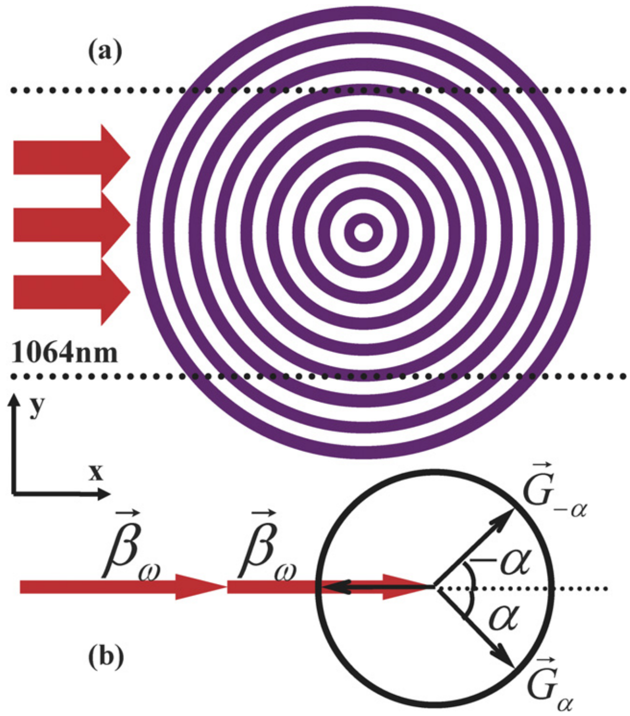

Figure 2. (a) Simplified layout of the case in which the pump passed through the center of the annular domain structure with a diameter of 4 mm in the experiment. The violet and white circles represent positive and negative domains, respectively. (b) The available reciprocal vectors $\vec{G}_{\alpha(-\alpha)}$ involved in the interaction.

in which $\vec{\beta}_\omega$ is the propagation constant of the TM_0 modes at 1064 nm, $\vec{G}_{\alpha(-\alpha)}$ are the circularly-distributed reciprocal vectors with the orientation angle $\alpha(-\alpha)$ between the reciprocal vectors and the x axis, $\vec{k}_{2\omega}$ is the wave vector of the second harmonic (SH) wave in the substrate and θ is the Cerenkov angle.

On the screen, we could clearly see a green ellipse-like shape with two spots and two green arcs, which is shown in figure 3(a). The green spot on top is Cerenkov SHG induced by the reciprocal vectors $\vec{G}_\pi$, while the spot at the bottom resulted from direct Cerenkov SHG, in which non-reciprocal vectors were involved [6]. The arcs ① and ② were two different types of scattering-involved Cerenkov SHG [27, 28]. Since a proton-exchanged z-cut LT waveguide only maintains TM modes, the fundamental wave, its elastic-scattering wave and scattering-involved Cerenkov interaction (the arcs ① and ②) are all z-polarized. Actually, when Cerenkov SHG occurs, a prerequisite condition ($\vec{v}_p > \vec{v}'$) as shown below should be satisfied:

$$|\vec{k}_{2\omega}| > \left|\vec{\beta}_\omega + \vec{\beta}_\omega + \vec{G}_{\alpha(-\alpha)}\right|. \tag{2}$$

Thus, not all reciprocal vectors could participate in the interaction. For such a reason, in our experiment shown in figure 3(a), the green ellipse was not self-enclosed and had a gap on the bottom. It was found that when α was in the range of [0°, 54°], $\vec{G}_{\alpha(-\alpha)}$ could not meet the requirement above, according to our simulations shown in figure 3(b).

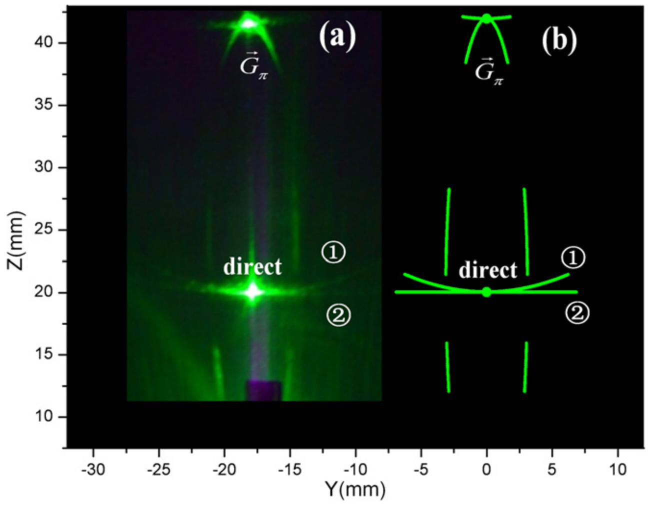

Figure 3. (a) Projection of the radiated SH pattern on the screen. The positive and negative numbers on the Y-axis represent the relative positions of the radiated SH spots in the y direction and the Z-axis represents the Cerenkov SH spot distribution in the z direction. (b) The calculated relative distributions of Cerenkov SH spots on the screen.

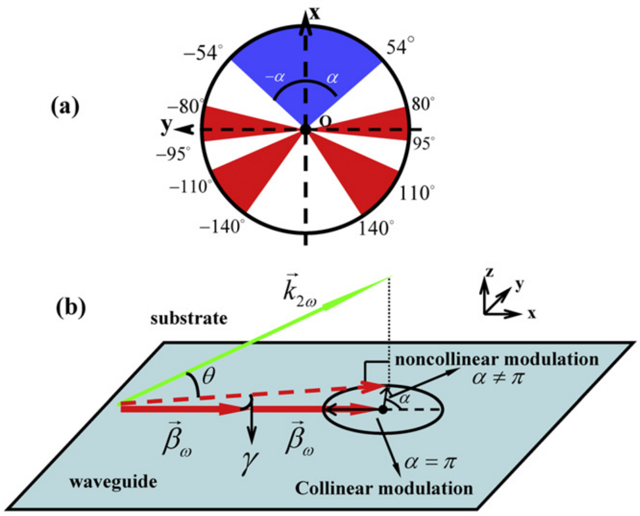

Figure 4. (a) Schematic diagram of the reciprocal vector distribution (the round face). The blue part represents the unsuitable reciprocal vectors and the red parts are the reciprocal vectors related to the absent positions of the radiated wave. (b) The phase-matching geometry including the collinear modulation and noncollinear modulation by the reciprocal vectors.

Considering the continuous distribution of $\vec{G}_{\alpha(-\alpha)}$, the modulated Cerenkov radiation should also be continuous. However, in our experiment we could clearly observe that parts of the green ellipse were absent and had approximately bilateral symmetry with the z-axis. The intensity of these absent parts was so weak that one hardly saw the Cerenkov radiation. As shown in figure 4, the whole round face represented the distribution of all of the reciprocal vectors provided by the domain annular poling and the blue part was the range of unsuitable reciprocal vectors discussed above. Based on our calculations shown in figure 3(b), we obtained the range of reciprocal vectors $\vec{G}_{\alpha(-\alpha)}$ related to such absent places, which were marked as the red portions of figure 4. These four red parts had bilateral symmetry with the x-axis and the corresponding α were within the range of [80°, 95°] and [110°, 140°]. The larger α induced a greater number of absent places, because when a reciprocal vector with larger orientation angle was involved in the interaction, $\vec{v}_p$of the nonlinear polarization would be accelerated more so as to emit a bigger Cerenkov angle.

For the interaction involving the 1st-order reciprocal vectors (i.e. the green ellipse around the direct Cerenkov spot), following coupled-mode theory via a nondepletion approximation [3], the SH power is:

$$P(2\omega) \propto L\,|\kappa|^2 {d_{\text{eff}}}^2 P^2(\omega), \tag{3}$$

in which L is the waveguide length, κ is the overlap between the radiated SH wave and the pump, d_{eff} is the effective nonlinear coefficient and $P(\omega)$ is the pump power. Using the same sample and pump power in our experiment, $P(2\omega)$ depended chiefly upon the overlap which could be expressed as:

$$\kappa(\alpha) = \frac{\left[y \cdot \int |\Phi_1|^2 \mathrm{d}z\right]^2 \cdot \left[y \cdot \int |\Phi_2(\alpha)|^2 \mathrm{d}z\right]}{\left[y \cdot \int \Phi_2(\alpha)^* \cdot {\Phi_1}^2 \mathrm{d}z\right]^2}, \tag{4}$$

in which y is the beam width of the pump, and Φ_1, and $\Phi_2(\alpha)$ are field distributions of the guided pump mode and SH radiated mode, respectively. Since collinear modulation had the largest overlap, the spot with $\vec{G}_\pi$ participating on top of the green ellipse was the brightest. Due to the noncollinear reciprocal vectors shown in figure 4(b), the radiated SH wave would deviate from the x–z plane, and accordingly led to the decrease of the overlap. When α was 90°, the deviation (angle γ) was the largest. Another thing that should be noted is that Cerenkov SHG itself is a noncollinear phase-matching process, in which the overlap is also related to the Cerenkov angle θ. As α increased, θ monotonously increased. Therefore, we took both aspects into consideration to simulate their effect on the overlap. As shown in figure 5, we found that the overlap was smallest at $\alpha = 122.5°$. I It was also found that when the reciprocal vectors in the range near 122.5° participated in the interaction, κ was still quite small, so that the radiated SH wave was hardly seen, which induced the absent parts on top of the ellipse shown in figure 3(a).

When the modulated condition was much closer to the collinear case ($\alpha = \pi$), the overlap was much bigger, as seen in figure 5. We measured the intensity of the SH wave involving reciprocal vectors with α from 140° to 175°, as shown in figure 6. The SH intensity became larger with increasing of the angle α, which was in good agreement with our simulations. If we carefully observed figure 3, it was found that there was another weak part near the direct Cerenkov spot and the corresponding reciprocal vectors were in

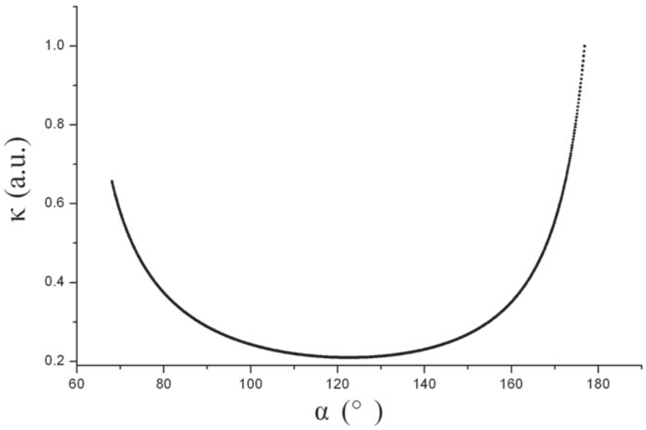

Figure 5. Relationship between the overlapping and reciprocal vectors with different orientation angles.

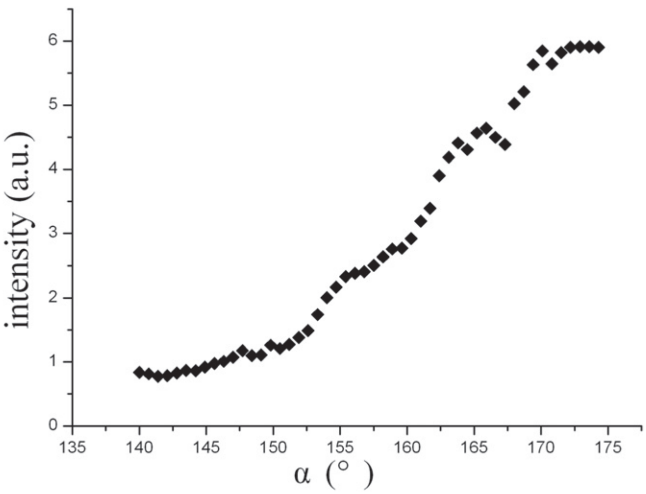

Figure 6. Dependence of radiated SH intensity on the reciprocal vectors with orientation angle in the range [140°, 175°].

the range [80°, 95°], according to our calculations. Based on the simulations in figure 5, the overlaps with these reciprocal vectors involved were not too small to generate SH radiation. Actually, in the experiment, we could observe another frequency doubling pattern near the bottom of the nonlinear Cerenkov SH (figure 3), as shown in figure 7(a), which is the SHG of Raman–Nath diffraction. The phase-matching condition shown in figure 7(b) could be expressed as:

$$\left|\vec{\beta}^{i}_{2\omega}\right| \sin\theta_i = \left|i\vec{G}_{\pm\pi/2}\right|, \tag{5}$$

Compared with Cerenkov SHG which only has a type of longitudinal phase-matching, frequency-doubling of Raman-Nath diffraction just follows transverse phase-matching conditions. As a result of the limit effect of the waveguide, nonlinear diffraction spots were elongated along the direction of the z-axis on the screen. Based on our calculations, the efficiency of nonlinear diffraction is much larger than that of nonlinear Cerenkov interaction under the same conditions. For the above discussed weak part of the Cerenkov SH image

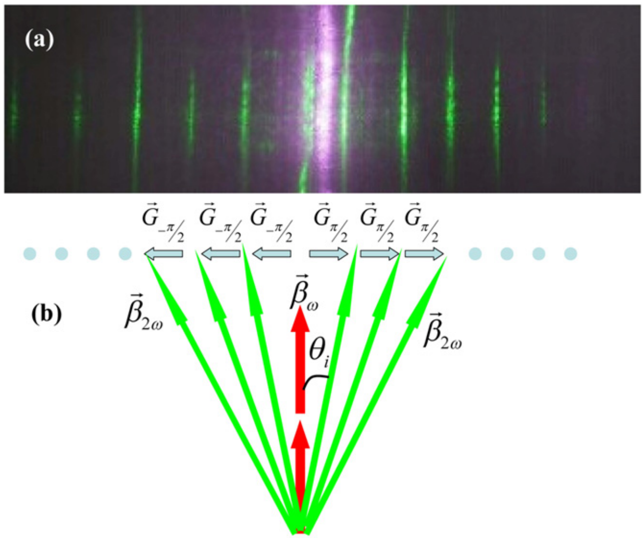

Figure 7. (a) Frequency-doubling of nonlinear diffraction in the waveguide (emitting on the screen). (b) The phase-matching geometry of the nonlinear diffraction.

in figure 3, we speculated that there was a competition between nonlinear Cerenkov interaction and nonlinear diffraction. For the reciprocal vectors in the range [80°, 95°], the domain walls were closer to parallel in such a situation, so nonlinear diffraction occurred more easily and the effect was more obvious. Most of the fundamental wave power was involved in nonlinear diffraction, which resulted in the nonlinear Cerenkov SH hardly being generated under such a condition, i.e. the weak part near the direct Cerenkov spot was generated, as shown in figure 3.

4. Conclusion

In summary, we have realized and experimentally characterized the modulation of Cerenkov SHG in a $LiTaO_3$ waveguide with an annular periodic-poled domain structure. Compared with other 2D structures, this structure with continuous rotation symmetry enables extremely wide modulation tolerance to phase velocity of a nonlinear polarization wave in a waveguide. On the other hand, the reciprocal vectors involved in the interaction had a threshold of orientation angle to meet the prerequisite condition of generating nonlinear Cerenkov radiation. The SH intensity dependence on the overlap between the radiated wave and the pump has also been studied. We demonstrated that the modulation of parts of the reciprocal vectors could induce a small overlap, so the SH radiation was too weak to been observed in the experiment. Our detailed discussions on Cerenkov SHG in such an annular-poling crystal will provide other researchers with a sound basis for later study, especially on the modulation of reciprocal vectors in other nonlinear Cerenkov processes, such as, sum-frequency generation, difference-frequency generation and so on.

Acknowledgments

This work was supported by the National Natural Science Foundations of China under Contract No. 11404167 and the China Postdoctoral Science Foundation (2015M581785).

References

[1] Tien P K, Ulrich R and Martin R J 1970 *Appl. Phys. Lett.* **17** 447
[2] Sanford N A and Connors J M 1989 *J. Appl. Phys.* **65** 1429
[3] Tamada H 1991 *IEEE J. Q. Electron.* **27** 502
[4] Li M J, De Micheli M, HE Q and Ostrowsky D B 1990 *IEEE J. Q. Electron.* **8** 1384
[5] Yamamoto K, Yamamoto H and Taniuchi T 1991 *Appl. Phys. Lett.* **58** 1227
[6] Chen C D, Lu J, Liu Y H, Hu X P, Zhao L N, Zhang Y, Zhao G, Yuan Y and Zhu S N 2011 *Opt. Lett.* **7** 1227
[7] Deng X W and Chen X F 2010 *Opt. Express* **18** 15597
[8] Ren H J, Deng X W, Zheng Y L, An N and Chen X F 2012 *Phys. Rev. Lett.* **108** 223901
[9] An N, Ren H J, Zheng Y L, Deng X W and Chen X F 2012 *Appl. Phys. Lett.* **100** 221103
[10] Armstrong J A, Bloembergen N, Ducuing J and Pershan P S 1962 *Phys. Rev.* **127** 1918
[11] Vaya M, Thyagarajan K and Kumar A 1998 *J. Opt. Soc. Am.* B **15** 1322
[12] Zhang Y, Gao Z D, Qi Z, Zhu S N and Ming N B 2008 *Phys. Rev. Lett.* **100** 163904
[13] Zhao X H, Zheng Y L, Ren H J, An N and Chen X F 2014 *Opt. Lett.* **39** 5885
[14] Karpinski P, Chen X, Shvedov V, Hnatovsky C, Grisard A, Lallier E, Davies B L, Krolikowski W and Sheng Y 2015 *Opt. Express* **23** 14903
[15] Xu P, Ji S H, Zhu S N, Yu X Q, Sun J, Wang H T, He J L, Zhu Y Y and Ming N B 2004 *Phys. Rev. Lett.* **93** 133904
[16] Saltiel S M, Neshev D N, Fischer R, Krolikowski W, Arie A and Kivshar Y S 2008 *Phys. Rev. Lett.* **100** 103902
[17] Saltiel S M, Neshev D N, Krolikowski W, Bloch N V, Arie A, Bang O and Kivshar Y S 2010 *Phys. Rev. Lett.* **104** 083902
[18] Vyunishev A M, Arkhipkin V G, Slabko V V, Baturin I S, Akhmatkhanov A R, Shur V Y and Chirkin A S 2015 *Opt. Lett.* **40** 4002
[19] Sheng Y, Saltiel S M, Krolikowski W, Arie A, Koynov K and Kivshar Y S 2010 *Opt. Lett.* **35** 1317
[20] Wang W J, Sheng Y, Kong Y F, Arie A and Krolikowski W 2010 *Opt. Lett.* **35** 3790
[21] Ayoub M, Roedig P, Imbrock J and Denz C 2011 *Appl. Phys. Lett.* **99** 241109
[22] Sheng Y, Wang W J, Shiloh R, Roppo V, Kong Y F, Arie A and Krolikowski W 2011 *Appl. Phys. Lett.* **98** 241114
[23] Chen C D, Hu X P, Xu Y L, Xu P, Zhao G and Zhu S N 2012 *Appl. Phys. Lett.* **101** 071113
[24] Bloch N V, Davidovich T, Ellenbogen T, Padowicz A G and Arie, A 2010 *Opt. Lett.* **35** 2499
[25] Kasimov D, Arie A, Winebrand E and Rosenman G 2006 *Opt. Express* **14** 9371
[26] Saltiel S, Krolikowski W, Neshev D and Kivshar Y S 2007 *Opt. Express* **15** 4132
[27] Zhang Y, Hu X P, Zhao G, Zhu S N and Xiao M 2009 *J. Phys. D: Appl. Phys.* **42** 215103
[28] Chen C D, Zhang Y, Zhao G, Hu X P, Xu P and Zhu S N 2012 *J. Phys. D: Appl. Phys.* **45** 405101